Energy Conversion and Management 105 (2015) 127–138

Contents lists available at ScienceDirect

Energy Conversion and Management

journal homepage: www.elsevier.com/locate/enconman

A comparative exergoeconomic analysis of different ORC configurations for binary geothermal power plants

V. Zare *

Faculty of Mechanical Engineering, Urmia University of Technology, Urmia, Iran

ARTICLE INFO

Article history:
Received 20 April 2015
Accepted 28 July 2015
Available online 4 August 2015

Keywords:
Binary power plant
Exergoeconomics
Geothermal energy
Organic Rankine cycle
Optimization

ABSTRACT

The main goal of this research is to investigate and compare the performance of three configurations of organic Rankine cycle (ORC) for binary geothermal power plants from the viewpoints of both thermodynamics and economics. The considered configurations are: Simple organic Rankine cycle (S-ORC), Regenerative organic Rankine cycle (R-ORC) and organic Rankine cycle with Internal Heat Exchanger (ORC-IHE). To assess the cycles' performances, thermodynamic and exergoeconomic models are developed and a parametric study is carried out prior to the optimization with respect to the total product cost minimization, as the objective function. Also, a profitability evaluation of the investigated systems is performed based on the total capital investment and payback period. The results indicate that, from the thermodynamic point of view (first and second law efficiencies), the ORC-IHE has superior performance while from the economic viewpoint the S-ORC is the best case among the considered cycles.

© 2015 Elsevier Ltd. All rights reserved.

1. Introduction

In recent years, renewable energy resources have received enormous interest due to the electricity market realities and the environmental concerns. Among the renewable energies, geothermal one is a promising source due to its consistency and reliability. In the context of geothermal power generation, organic Rankine cycles (ORCs) are adopted as eligible technologies since they have some promising features such as configuration simplicity, components availability and better economics. Among the major types of geothermal power plants, the binary units based on ORCs are becoming increasingly common [1] and some case studies are performed on performance evaluation of these plants in different countries [2–5].

Recently, some efforts have been made to investigate the performance of different configurations of ORC-based binary power plants. For some operating binary geothermal power plants, the second law analysis is reported by Dipippo [6], who showed that binary plants can operate with high second law efficiencies (40% or higher) even when a low-temperature geothermal fluid is available. Kanoglu et al. [7] performed exergy analysis for an existing 27 MW binary geothermal power plant, with isobutane as the working fluid and liquid-dominated heat source at 160 °C. Their results showed that, the energy and exergy efficiencies are 10.2% and 33.5%, respectively. For a simple ORC power cycle utilizing low-temperature geothermal source, an optimum cost-effective design criterion was presented by Madhawa et al. [8], where the ratio of the total heat exchangers' area to net power output is used as the objective function. The results revealed that, among the considered working fluids, ammonia has lower objective function, but not necessarily higher cycle efficiency. Yari [9] conducted a comparative study of different geothermal power plants, based on the exergy analysis, for high-temperature geothermal resources. The potential of ORC for the exploitation of low-medium enthalpy geothermal brines is investigated by Astolfi et al. [10], from thermodynamic and economic viewpoints. They reported that, techno-economic optimization provides results different from the ones obtained by thermodynamic analysis, confirming its primary importance in the optimization of ORC plants. Walraven et al. [11] analyzed the performance of different ORC types and the Kalina cycle for low-temperature (100–150 °C) geothermal heat sources. The results indicated that, trans-critical and multi-pressure subcritical ORCs are in most cases the best performing cycles and they outperform the investigated Kalina cycle. Using real thermodynamic and cost data, exergy and exergoeconomic analyses of the 9.5 MW Dora II geothermal power plant, located in Turkey, are carried out by Ganjehsarabi et al. [12]. The results showed that, the unit cost of produced electricity and the unit exergetic cost of geothermal fluid are 5.3 cents/kW h and 1.67 cents/kW h, respectively. Heberle et al. [13] presented an exergoeconomic analysis of a simple ORC-based binary power plant with isobutane and

* Tel.: +98 44 31980228.
E-mail address: v.zare@uut.ac.ir

http://dx.doi.org/10.1016/j.enconman.2015.07.073
0196-8904/© 2015 Elsevier Ltd. All rights reserved.

Nomenclature

$\dot{C}$	cost rate ($\$ h^{-1}$)
c	specific exergy cost ($\$ GJ^{-1}$)
$\dot{E}$	exergy rate (kW)
h	specific enthalpy (kJ kg^{-1})
i_r	interest rate
k	thermal conductivity (kW m^{-1} K^{-1})
$\dot{m}$	mass flow rate (kg s^{-1})
P	pressure (bar)
Pr	Prandtl number
Nu	Nusselt number
$\dot{Q}$	heat transfer rate (kW)
Re	Reynolds number
s	specific entropy (kJ kg^{-1} K^{-1})
T	temperature (°C or K)
U	overall heat transfer coefficient (kW m^{-2} K^{-1})
V	velocity (m s^{-1})
w	width of the plate (m)
$\dot{W}$	power (kW)
x	extraction ratio
Z	investment cost of components ($)
$\dot{Z}$	investment cost rate of components ($\$ h^{-1}$)

Subscripts and abbreviations

0	ambient
A	heat transfer surface area (m^2)
AR	annual revenue
a	actual process
CI	capital investment
CRF	capital recovery factor
CD	condenser
D	destruction
EV	evaporator
F	fuel
GB	geothermal Brine
IHE	internal heat exchanger
l	liquid
OF	organic Fluid
OFH	open feed heater
OM	operation and maintenance
ORC	organic Rankine cycle
ORC-IHE	organic Rankine cycle with Internal Heat Exchanger
P	pump
ph	physical
PP	pinch point, payback period
PEC	purchased equipment cost
R-ORC	regenerative organic Rankine cycle
s	isentropic process
S-ORC	Simple organic Rankine cycle
Sup	superheater
TCI	total capital investment
v	vapor
w	water

Greek symbols

τ	annual plant operation hours
η_I	first law efficiency
ε	effectiveness
η_{II}	second law efficiency
η_P	pump isentropic efficiency
η_T	turbine isentropic efficiency
α	convection heat transfer coefficient (kW m^{-2} K^{-1})

isopentane as the working fluids. They reported that, under the exergoeconomic optimization conditions, isobutane with a minimum temperature difference of 3 K at evaporation and 7 K at condensation is favorable. For an existing ORC utilizing low temperature geothermal source, with isobutane as the working fluid, a thermodynamic model is developed by Ghasemi et al. [14] and validated by approximately 5000 measured data in a wide range of ambient temperatures. Zhang et al. [15] examined the thermodynamic and economic performance of both subcritical and trans-critical ORC for low-temperature geothermal sources. The results revealed that, working fluids favored by the thermal and exergy efficiencies are: R123, R600, R245fa, R245ca and R600a, while low levelized cost value is observed for R152a, R600, R600a, R134a, R143a, R125. A sensitivity analysis of system parameters on the ORC performance, for binary geothermal power plants, is performed by Liu et al. [16] and the effects of such parameters as; working fluid, superheat temperature, pinch temperature difference in evaporator and condenser and evaporation temperature are studied. They reported that, the evaporation temperature has significant effect on the thermodynamic and economic performance of the ORC. Zhang et al. [17] analyzed the thermodynamic performance of three types of the ORC (subcritical, superheated and trans-critical) for four geofluid temperatures. Their results proved that, the thermo-physical properties of the working fluids and the cycle type are of the key factors affecting the power plant performance. Thermodynamic and economic analyses on a novel-type geothermal regenerative ORC is presented by El-Emam et al. [18]. Parametric studies are carried out to investigate the effect of operating parameters on the system performance and an optimization is performed based on the heat exchangers total surface area. Their results revealed that, an increase of the dead state temperature increases the cost rate of the exergy destruction in the system.

To improve the binary plant performance, recently some efforts have been devoted to propose and investigate novel configurations of ORCs such as ORC with internal heat exchanger and regenerative ORC [9,18–23]. The objective of the present paper is to analyse and compare these configurations with the well-known simple ORC from the exergoeconomic perspective. The previous studies are mostly focused on thermodynamic analysis and revealed that the mentioned novel configurations outperform the simple ORC in terms of thermodynamic efficiency. The assessment of conversion of simple ORC into the novel configurations and relative increase in cost is not discussed enough. The current work intends to present a comparative analysis of the three configurations in terms of thermodynamics and economics at their cost-optimal design point. The results will be helpful to visualize the relative increase in cost of simple ORC conversion to the other configurations. In most of the above mentioned references, often certain assumptions are made in the analyses (like fixed values for condenser temperature, pinch point temperature difference, internal heat exchanger effectiveness, the ratio of extracted vapor in regenerative cycle) and no superheat is assumed at turbine inlet. However, in the present study the effects of all the potential decision variables and operating conditions are comprehensively assessed on thermodynamic and economic performances. A review of the previous literature reveals that, there is no sufficient knowledge on investigating and comparing the exergoeconomic performance of the mentioned ORC configurations for binary power plants. The exergoeconomic analysis is a technique which combines the exergy and economic

analyses to provide essential information for evaluating the cost of individual exergy streams (including the system products) as well as the cost of inefficiencies.

2. System description and assumptions

Among geothermal energy resources, the low and medium-temperature water-dominated fields are the most abundant available in the world. To exploit these resources, binary power plants are the best energy conversion systems, from both technical and environmental viewpoints [24]. These systems employ a secondary organic working fluid within a closed Rankine cycle referred to as organic Rankine cycle. The schematic diagrams of three ORC configurations, considered in the present study, are presented in Fig. 1. The Simple organic Rankine cycle (S-ORC) consists of four major components; evaporator (and superheater), turbine, condenser and pump. As Fig. 1(a) indicates, in the S-ORC the organic working fluid passing through the evaporator (and superheater) absorbs thermal energy from the geothermal brine. The working fluid is then expanded in the turbine to produce power and after that it is cooled down and condensed in the condenser before being pumped again to the evaporator.

In contrast to the conventional steam power plants, for most organic fluids the expansion in the turbine ends up in vapor phase above the condenser temperature instead of the two-phase region. Therefore, for performance improvement of the S-ORC, an Internal Heat Exchanger (IHE) can be employed to recover some part of the energy content of the turbine exiting stream. This configuration is referred to as ORC with IHE, as illustrated in Fig. 1(b).

Another alternative to improve the S-ORC performance is to extract a fraction of the working fluid between the turbine stages for feed heating before the evaporator. Fig. 1(c) shows this configuration of the ORC which is called Regenerative organic Rankine cycle (R-ORC).

The following assumptions are made in the analyses of the systems:

1. The systems operate in a steady state condition.
2. Changes in kinetic and potential energies are neglected.
3. The pumps and the turbines operate adiabatically with appropriate isentropic efficiencies as given in Table 6.
4. Pressure losses are neglected through the heat exchangers and in the pipelines.
5. A water-dominated reservoir is considered for the geothermal field and saturated liquid state is assumed for the geothermal brine.

2.1. Working fluid selection

Regarding the ORC working fluids, previous studies have indicated that good working fluids have the following characteristics [25,26]:

- High latent and specific heat.
- High densities in both liquid and gas phase.
- Moderate critical temperature and pressure.
- Moderate evaporating and condensing pressures.
- Excellent transport and heat transfer properties (like low viscosity and high thermal conductivity).
- Safety and chemical stability.
- Material capability and no corrosion.
- Market availability and cost.
- Environmentally benign (zero ODP and low GWP).

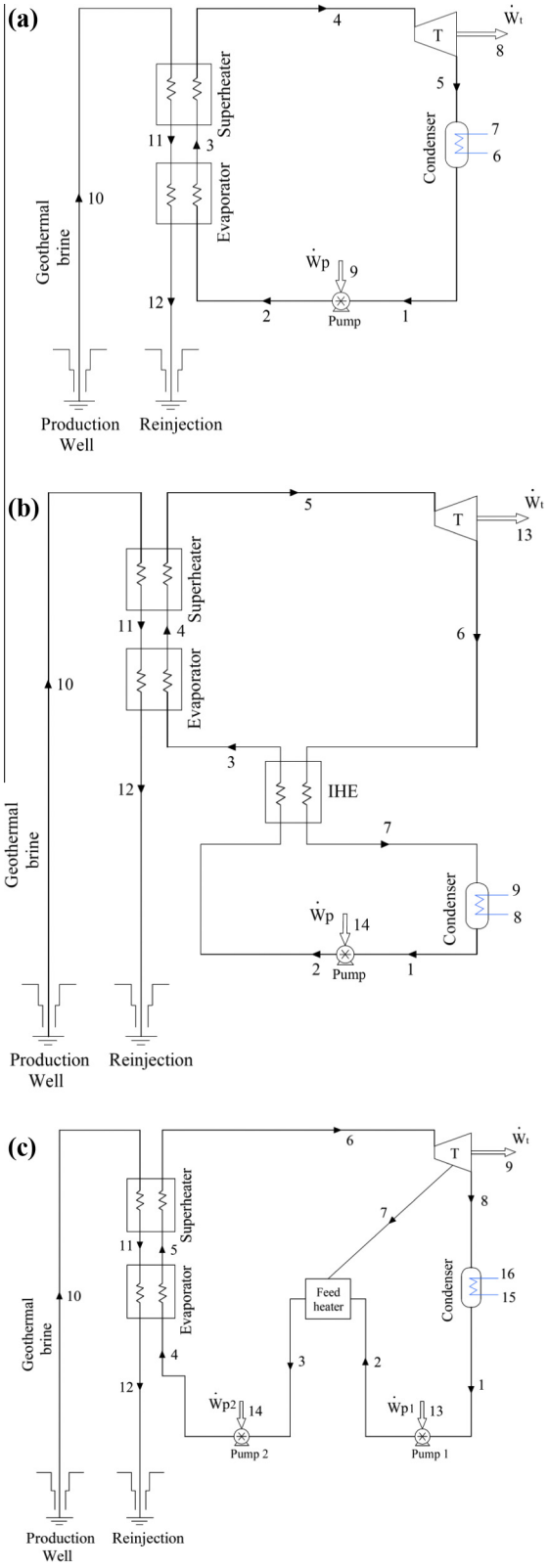

Fig. 1. Schematic diagrams of the binary geothermal power plants; (a): Simple organic Rankine cycle (S-ORC), (b): organic Rankine cycle with Internal Heat Exchanger (ORC-IHE); (c): Regenerative organic Rankine cycle (R-ORC).

The working fluid properties have an important role on the ORC performance. In the present work, regarding the heat source temperature and fluid properties, four candidate working

fluids, namely Isobutane, n-pentane, R245fa and R152a are selected and the performances of the cycles are optimized for each of them. However, the results of parametric study are given for Isobutane. The selected working fluids are among those which widely adopted in the ORC systems for geothermal power generation, and besides a zero ODP they are the recommended fluids for application [16,24,27]. There are a number of operating geothermal power plants in which Isobutane and n-pentane are aptly employed as the working fluid [6,7,12]. Also, previous researches have shown that R152a has good characteristics, from the economic viewpoint, for a subcritical ORC utilizing geothermal energy [15].

3. Thermodynamic analysis

The pre-described systems are simulated by computer programs developed using the Engineering Equation Solver (EES) software. In simulating procedure, each system component is treated as a control volume for which the principles of mass conservation, first and second laws of thermodynamics are applied.

3.1. First law analysis

The schematic T–s diagrams for the three considered cycles are presented in Fig. 2. Simulation of the cycles and calculation of the performance parameters are carried out for a given value of geothermal brine mass flow rate. For the evaporator and condenser analysis, the pinch point assessment is an important factor on which the cycles' performances depend. The heat exchangers performances are assessed by fixing the pinch point temperature difference, as demonstrated by Fig. 2 for the case of S-ORC. Also, it is worth mentioning that the condenser temperature is related to the ambient temperature via the pinch point determination. The relations used in the first law analysis of the cycles are given in Table 1.

Based on the thermal energy input to the ORC, the thermal or first law efficiency of a binary geothermal power plant may be expressed as follows [7,9]:

$$\eta_I = \frac{\dot{W}_{net}}{\dot{Q}_{in}} = \frac{\dot{W}_{net}}{\dot{m}_{GB}(h_{10} - h_{12})} \tag{1}$$

3.2. Second law analysis

In evaluating the systems' performances, more attention is paid to the second law of thermodynamics as it provides more meaningful assessment. Considering the fact that the chemical exergy is canceled out in the exergy balance equations and ignoring the kinetic and potential exergies, the total exergy of a fluid stream can be written as:

$$\dot{E} = \dot{E}_{ph} = \dot{m}[(h - h_0) - T_0(s - s_0)] \tag{2}$$

Considering the transferred exergy from the geothermal brine to the organic fluid as the input exergy to the cycle, the exergy or second law efficiency of a binary geothermal power plant can be expressed as [7,9]:

$$\eta_{II} = \frac{\dot{W}_{net}}{\dot{E}_{in}} = \frac{\dot{W}_{net}}{\dot{m}_{GB}(\dot{E}_{10} - \dot{E}_{12})} \tag{3}$$

Applying the exergy balance equation on each system component, the exergy destruction rate within that component can be calculated as:

$$\dot{E}_{D,k} = \sum \dot{E}_{in,k} - \sum \dot{E}_{out,k} \tag{4}$$

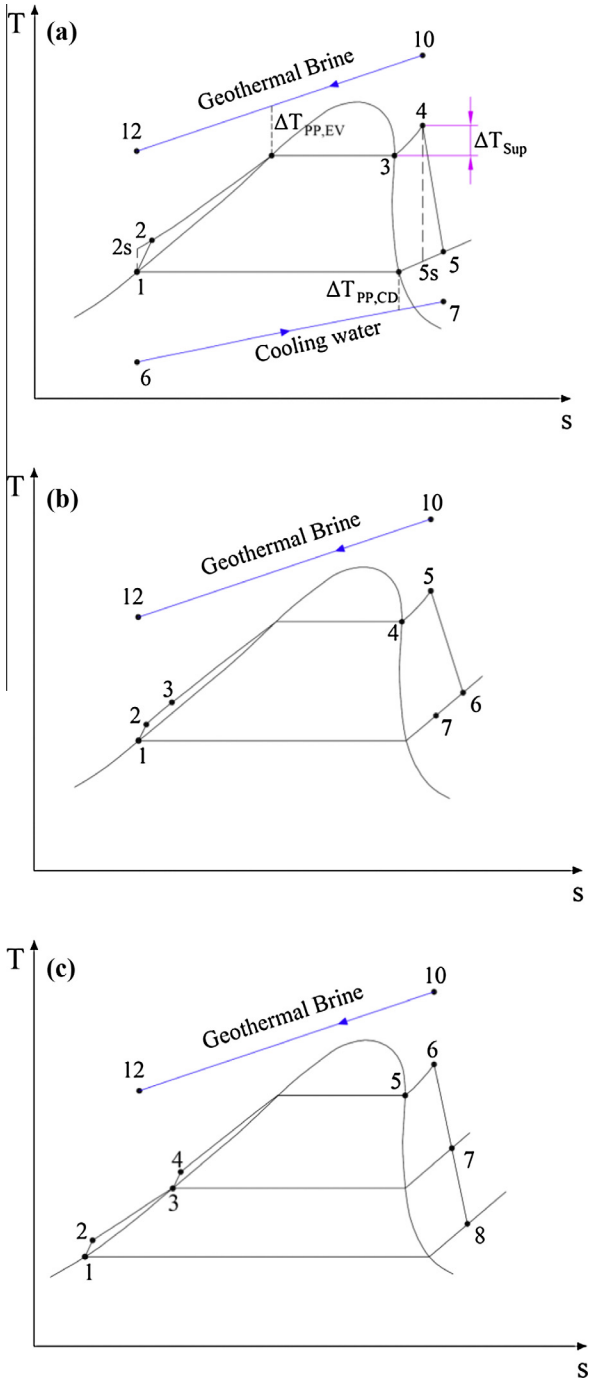

Fig. 2. Schematic T–s diagrams of the cycles and illustration of pinch point for the S-ORC; (a): S-ORC, (b): ORC-IHE; (c): R-ORC.

4. Exergoeconomic analysis

During the last two decades, different methodologies have been developed for exergoeconomic analysis of thermal systems. Among these methodologies, the specific exergy costing method (SPECO), introduced by Lazzaretto and Tsatsaronis [28], has been widely applied to energy intensive systems by the researchers in the field of thermoeconomics. The SPECO theory establishes a logical method for determining the cost rates and the specific exergy costs of streams in a thermal system. This methodology is used in the present paper to analyse and compare the exergoeconomic performance of the binary geothermal power plants.

Table 1
Relations used in first law analysis of the considered cycles.

Component	Energy equations		
	S-ORC	ORC-IHE	R-ORC
Pump	$\eta_P = \frac{w_s}{w_a} = \frac{v_1(P_2-P_1)}{h_2-h_1}$ $\dot{W}_P = \dot{m}_1(h_2-h_1)$	$\eta_P = \frac{w_s}{w_a} = \frac{v_1(P_2-P_1)}{h_2-h_1}$ $\dot{W}_P = \dot{m}_1(h_2-h_1)$	$\eta_{P1} = \frac{w_s}{w_a} = \frac{v_1(P_2-P_1)}{h_2-h_1}$ $\dot{W}_{P1} = \dot{m}_1(h_2-h_1)$ $\eta_{P2} = \frac{w_s}{w_a} = \frac{v_3(P_4-P_3)}{h_4-h_3}$ $\dot{W}_{P2} = \dot{m}_3(h_4-h_3)$
Evaporator	$\dot{Q}_{EV} = \dot{m}_1(h_3-h_2)$ $= \dot{m}_{10}(h_{11}-h_{12})$	$\dot{Q}_{EV} = \dot{m}_1(h_4-h_3)$ $= \dot{m}_{10}(h_{11}-h_{12})$	$\dot{Q}_{EV} = \dot{m}_3(h_5-h_4)$ $= \dot{m}_{10}(h_{11}-h_{12})$
Superheater	$\dot{Q}_{Sup} = \dot{m}_1(h_4-h_3)$ $= \dot{m}_{10}(h_{10}-h_{11})$	$\dot{Q}_{Sup} = \dot{m}_1(h_5-h_4)$ $= \dot{m}_{10}(h_{10}-h_{11})$	$\dot{Q}_{Sup} = \dot{m}_3(h_6-h_5)$ $= \dot{m}_{10}(h_{10}-h_{11})$
Turbine	$\eta_T = \frac{w_a}{w_s} = \frac{h_4-h_5}{h_4-h_{5s}}$ $\dot{W}_T = \dot{m}_1(h_4-h_5)$	$\eta_T = \frac{w_a}{w_s} = \frac{h_5-h_6}{h_5-h_{6s}}$ $\dot{W}_T = \dot{m}_1(h_5-h_6)$	$\eta_T = \frac{w_a}{w_s} = \frac{h_6-h_7}{h_6-h_{7s}}$ $\dot{W}_T = \dot{m}_3h_6 - \dot{m}_7h_7 - \dot{m}_1h_8$
Condenser	$\dot{Q}_{CD} = \dot{m}_1(h_5-h_1)$ $= \dot{m}_6(h_7-h_6)$	$\dot{Q}_{CD} = \dot{m}_1(h_7-h_1)$ $= \dot{m}_8(h_9-h_8)$	$\dot{Q}_{CD} = \dot{m}_1(h_8-h_1)$ $= \dot{m}_{15}(h_{16}-h_{15})$
IHE	–	$\varepsilon_{IHE} = \frac{T_6-T_7}{T_6-T_2}$ $\dot{Q}_{IHE} = \dot{m}_1(h_3-h_2)$ $= \dot{m}_1(h_6-h_7)$	–
OFH	–	–	$\dot{m}_1h_2 = \dot{m}_7h_7 + \dot{m}_3h_3$ $x = \dot{m}_7/\dot{m}_3$

To perform an exergoeconomic analysis, a cost balance equation along with sufficient number of auxiliary equations, are applied to each system component. The cost balance equation can be expressed as [29]:

$$\sum \dot{C}_{out,k} = \sum \dot{C}_{in,k} + \dot{Z}_k \tag{5}$$

where $\dot{C}$ is the cost rate associated with the outlet and inlet exergy streams and $\dot{Z}$ is the total cost rate associated with capital investment and operation and maintenance costs for the kth component. The cost rates associated with the stream of matter, power and heat can be expressed as a function of specific exergy costs as follows:

$$\begin{aligned} \dot{C}_i &= c_i\dot{E}_i \\ \dot{C}_w &= c_w\dot{W} \\ \dot{C}_q &= c_q\dot{E}_q \end{aligned} \tag{6}$$

The $\dot{Z}$ term for the kth component can be written as:

$$\dot{Z}_k = \dot{Z}_k^{CI} + \dot{Z}_k^{OM} \tag{7}$$

The annual levelized capital investment, for the kth component, may be expressed as [29,30]:

$$\dot{Z}_k^{CI} = \left(\frac{CRF}{\tau}\right)Z_k \tag{8}$$

where CRF and τ are the capital recovery factor and the annual plant operation hours, respectively. The CRF is a function of the interest rate, i_r, and the number of years of the plant operation, n [30]:

$$CRF = \frac{i_r(1+i_r)^n}{(1+i_r)^n - 1} \tag{9}$$

The cost balance and auxiliary equations, for each component of the considered ORC plants, are given in Table 2.

4.1. Investment costs of the system components

For the exergoeconomic analysis, appropriate cost functions must be formulated for the investment costs of the equipments. These formulas are expressed as functions of suitable thermodynamic variables. For the considered systems, the purchased equipment cost (PEC) for different components are listed in Table 3.

For the heat exchangers, the PEC is a function of heat transfer surface area (A) and the construction material. All the heat exchangers are assumed to be made of carbon steel as it has good chemical compatibility with both geothermal brine and organic working fluids [31]. Using the LMTD method, the heat transfer process in heat exchangers is modeled as:

$$\dot{Q}_k = U_kA_k\Delta T_k^{lm} \tag{10}$$

where U_k is the overall heat transfer coefficient and ΔT_k^{lm} is the logarithmic mean temperature difference. The evaporator, condenser and internal heat exchanger are assumed to be shell and plate type heat exchangers since the high heat transfer coefficient of these heat exchangers results in more compactness, especially with the relatively low temperatures of the heat sources in geothermal ORCs [8,18]. The specifications of the heat exchangers used in the present work are given in Table 4.

Assuming negligible fouling effects, the overall heat transfer coefficient, can be expressed as:

$$\frac{1}{U} = \frac{1}{\alpha_{OF}} + \frac{t}{k} + \frac{1}{\alpha_w} \tag{11}$$

where α_{OF} and α_w are the convection heat transfer coefficients of the organic fluid and water, respectively. Also, t and k are the thickness and thermal conductivity of the heat exchanger plate material. The convection heat transfer coefficients can be calculated using Nusselt number as follows:

$$Nu = \frac{\alpha D_{eq}}{k} \tag{12}$$

where D_{eq} denotes the approximate diameter equals to twice of the heat exchanger's plate clearance [18]. For the water side heat transfer coefficient the following correlation is used to evaluate Nusselt number [18]:

$$Nu = 0.04Re^{0.8}Pr^{0.33} \tag{13}$$

where Re and Pr are Reynolds and Prandtl numbers. The velocity of the water inside the heat exchangers can be calculated as follows:

$$V = \frac{\dot{V}}{w \cdot \delta x \cdot N} \tag{14}$$

where $\dot{V}$ is the water volumetric flow rate, w, δx and N are the width of the plate, the clearance at the water side and the number of plates, respectively.

The following correlations are used to evaluate the organic fluid heat transfer coefficient at the evaporator of the ORCs [8,18]:

Table 2
Cost balance and auxiliary equations for the cycles' components.

Component	Cost balance and auxiliary equations		
	S-ORC	ORC-IHE	R-ORC
Evaporator	$\dot{C}_3 + \dot{C}_{12} = \dot{C}_2 + \dot{C}_{11} + \dot{Z}_{EV}$ $c_{12} = c_{11}$	$\dot{C}_4 + \dot{C}_{12} = \dot{C}_3 + \dot{C}_{11} + \dot{Z}_{EV}$ $c_{12} = c_{11}$	$\dot{C}_5 + \dot{C}_{12} = \dot{C}_4 + \dot{C}_{11} + \dot{Z}_{EV}$ $c_{12} = c_{11}$
Superheater	$\dot{C}_4 + \dot{C}_{11} = \dot{C}_3 + \dot{C}_{10} + \dot{Z}_{Sup}$ $c_{10} = c_{11}$	$\dot{C}_5 + \dot{C}_{11} = \dot{C}_4 + \dot{C}_{10} + \dot{Z}_{Sup}$ $c_{10} = c_{11}$	$\dot{C}_6 + \dot{C}_{11} = \dot{C}_5 + \dot{C}_{10} + \dot{Z}_{Sup}$ $c_{10} = c_{11}$
Turbine	$\dot{C}_5 + \dot{C}_8 = \dot{C}_4 + \dot{Z}_T$ $c_4 = c_5$	$\dot{C}_6 + \dot{C}_{13} = \dot{C}_5 + \dot{Z}_T$ $c_6 = c_5$	$\dot{C}_7 + \dot{C}_8 + \dot{C}_9 = \dot{C}_6 + \dot{Z}_T$ $c_8 = c_6$ $c_7 = c_6$
Condenser	$\dot{C}_1 + \dot{C}_7 = \dot{C}_5 + \dot{C}_6 + \dot{Z}_{CD}$ $c_6 = 0$	$\dot{C}_1 + \dot{C}_9 = \dot{C}_7 + \dot{C}_8 + \dot{Z}_{CD}$ $c_8 = 0$	$\dot{C}_1 + \dot{C}_{16} = \dot{C}_8 + \dot{C}_{15} + \dot{Z}_{CD}$ $c_{15} = 0$
Pump	$\dot{C}_2 = \dot{C}_9 + \dot{C}_1 + \dot{Z}_P$ $c_9 = c_8$	$\dot{C}_2 = \dot{C}_{14} + \dot{C}_1 + \dot{Z}_P$ $c_{14} = c_{13}$	$\dot{C}_2 = \dot{C}_{13} + \dot{C}_1 + \dot{z}_{P1}$ $c_{13} = c_9$ $\dot{C}_4 = \dot{C}_3 + \dot{C}_{14} + \dot{Z}_{P2}$ $c_{14} = c_9$
IHE	–	$\dot{C}_3 + \dot{C}_7 = \dot{C}_2 + \dot{C}_6 + \dot{Z}_{Sup}$ $c_6 = c_7$	–
OFH	–	–	$\dot{C}_3 = \dot{C}_2 + \dot{C}_7 + \dot{Z}_{OFH}$

Table 3
Purchased equipment cost functions for systems' equipments.

System component	Purchased equipment cost	Refs.
Turbine	$log_{10}(PEC) = 2.6259 + 1.4398 log_{10}(\dot{W}_T) - 0.1776 (log_{10}(\dot{W}_T))^2$	[18]
Pump	$log_{10}(PEC) = 3.3892 + 0.0536 log_{10}(\dot{W}_P) + 0.1538 (log_{10}(\dot{W}_P))^2$	[18]
Heat exchangers	$PEC = 10000 + 324 (A_{EV})^{0.91}$	[31]
Open feed heater	$PEC = (527.7/397)^{1.70} \times \dot{C}$ $log_{10}(\dot{C}) = 4.20 - 0.204 log_{10}(\dot{V}) + 0.1245 (log_{10}(\dot{V}))^2$	[19]

Table 4
Heat exchangers specifications [18].

Parameter	Value
Heat transfer surface length (mm)	1465
Width of the plate (mm)	605
Clearance (mm)	5
Depth of the flute (mm)	1
Pitch of the flute (mm)	1
Plate thickness (mm)	0.9
Number of plates	200

$$Nu = \begin{cases} 1.18 (f_p X)^{0.919} \cdot H^{-0.834} \cdot (\rho_l/\rho_v)^{-0.448} & f_p X < 62 \\ 6.646 (f_p X)^{0.919} \cdot H^{-0.834} \cdot (\rho_l/\rho_v)^{-0.448} & f_p X > 62 \end{cases} \quad (15)$$

where H represents the ratio of sensible to latent heat, f_p is the pressure factor which is a function of the critical and the atmospheric pressure as follows:

$$f_p = \left[\left(\frac{P}{P_{cr}} \right)^3 + 1 \right] \left(\frac{P}{P_a} \right)^{0.7} \quad (16)$$

For the convection heat transfer coefficient, for the organic fluid at the condenser, the following correlation can be used [18]:

$$Nu = 2.018 \left(Bo \frac{p^2}{l \cdot \delta h} \right)^{-0.1} \cdot (Gr_l Pr_l / H)^{1/4} \quad (17)$$

where p, l and δh are the pitch of the flutes, the heat transfer length and the depth of the flutes, respectively. Also, the Bond number (Bo) and the Grashof number (Gr) are expressed as:

$$Bo = g \cdot \rho_l \cdot p^2 / \sigma \quad (18)$$

$$Gr = \left(\frac{g \cdot l^3}{v^2} \right) \left(\frac{\rho_l - \rho_v}{\rho_l} \right) \quad (19)$$

In conducting an economic analysis, estimation of the total capital investment (TCI) is the first step. The TCI consists of two parts: fixed capital investment and other outlays [29]. The fixed capital investment is the capital needed to purchase the land, build the facilities and purchase and install the required machinery and equipment. The other outlays are the sum of start-up costs, working capital costs, licensing and R&D funds. It is a common practice, in engineering economics, to estimate the TCI in terms of a percentage of the purchased equipment costs (PEC). For the systems' components in the present study, the total capital investment (TCI) is assumed to be 6.32 times of the PEC as given by Bejan [29] and used by other researchers [18]. The operation and maintenance costs for each component is assumed to be 20% of the PEC [13,18,29]. Since the drilling cost for geothermal power plants can be considered as a percentage of the TCI [18,32], it is taken as 50% of the TCI in the present work.

4.2. Validation of simulation models

To validate the developed models for the simulation of ORC systems, the available data in the literature were used. The comparisons of simulation results with those reported in literature are presented in Fig. 3(a and b) and Table 5. As can be seen, for both thermodynamic and economic criteria, there is a good agreement between the values of parameters calculated in the present paper and those published in literature [9,18,33]. Referring to Fig. 3(b), the largest difference of 3.5% is observed for exergy efficiency at evaporator pressure of 15 bar.

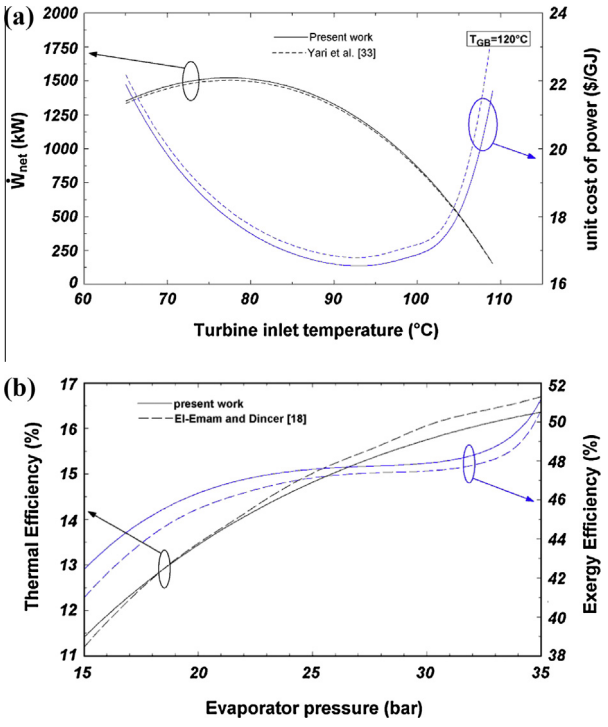

Fig. 3. Validation of developed model in the present study for; (a): S-ORC and (b): IHE-ORC.

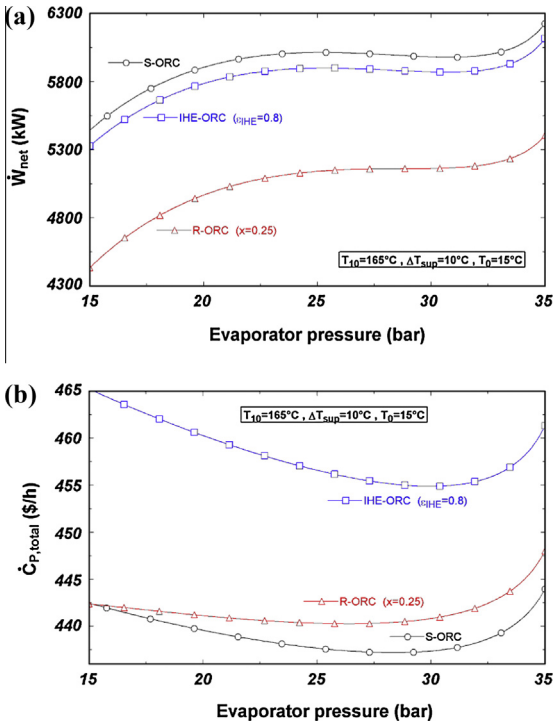

Fig. 4. Effects on the total product cost and net output power of evaporator pressure.

Table 5
Validation of developed model for IHE-ORC and R-ORC.

IHE-ORC			R-ORC		
Performance parameter*	Present work	[18]	Performance parameter	Present work	[9]
$T_{GB,in}(T_{10})$ (°C)	165	165	$T_{GB,in}(T_{10})$ (°C)	180	180
$T_{GB,out}(T_{12})$ (°C)	76.45	78.49	w_{net} (kJ/kg)	42.97	43.61
$\dot{m}_{GB}$ (kg/s)	82.16	84.36	η_I (%)	14.06	14.52
$\dot{m}_{OF}$ (kg/s)	76.09	78.06	η_{II} (%)	50.14	50.39
A_{EV} (m^2)	399.3	390.6	–	–	–
A_{CD} (m^2)	808.7	810.1	–	–	–
A_{IHE} (m^2)	124.2	124.8	–	–	–
η_I (%)	16.15	16.37	–	–	–
η_{II} (%)	48.54	48.8	–	–	–

* These values are calculated for 5 MWe net output power.

5. Results and discussion

For the investigated geothermal power plants, the considered assumptions and input parameters are given in Table 6.

A parametric study is performed to investigate the effects on the objective function of the decision variables. The results of parametric study are given for Isobutane as the working fluid. As an important objective in the optimization of energy systems, from the exergoeconomic viewpoint, is the total product cost minimization [34–36]. This parameter is selected as the optimization objective in the present study. It can be defined as:

$$\dot{C}_{P,total} = \dot{C}_F + \dot{Z}_{total} = \dot{C}_F + \dot{Z}^{CI}_{total} + \dot{Z}^{OM}_{total} \quad (20)$$

5.1. Results of parametric study

Fig. 4(a and b) shows the effects on the total product cost of the evaporator pressure, for the considered systems. Also, the values of net output power, $\dot{W}_{net}$, are presented in Fig. 4(a) as it is an important performance parameter in geothermal power plants. Referring to Fig. 4(b), there exist optimum values for evaporator pressure with which the $\dot{C}_{P,total}$ is minimized. Fig. 4 also reveals that the S-ORC has the lowest value of $\dot{C}_{P,total}$ while the lowest value of $\dot{W}_{net}$ belongs to R-ORC configuration, as expected.

Referring to Fig. 4(a), (which is given for a heat source temperature of 165 °C), at evaporator pressures of higher than about 33 bar the value of $\dot{W}_{net}$ increases. However, for a heat $\dot{W}_{net} = \dot{m}_3 w_{net}$ source temperature of 120 °C, as shown in Fig. 3(a), there is an optimum value of evaporator pressure at which the $\dot{W}_{net}$ is maximized. This different trend for net output power can be justified considering the variations of working flow mass flow rate with evaporator pressure presented in Fig. 5 for S-ORC case. As can be seen, for a geothermal brine temperature of 165 °C there is a slight increase in mass flow rate at evaporator pressures of higher than about 33 bar which results in an increase of $\dot{W}_{net} = \dot{m}_3 W_{net}$.

Fig. 6(a and b) shows the variations of total product cost and net output power of the cycles with vapor superheating degree (ΔT_{sup}) at turbine inlet. Referring to Fig. 6(b), the $\dot{C}_{P,total}$decreases first and

Table 6
The input data assumed in the simulation.

Parameter	Symbol	Value
Ambient (dead state) pressure	P_0 (bar)	1
Ambient (dead state) temperature	T_0 (°C)	15
Geothermal brine (heat source) temperature	$T_{GB}(T_{10})$ (°C)	160–170
Geothermal brine mass flow rate	$\dot{m}_{GB}$ (kg/s)	100
Turbine isentropic efficiency	η_T (%)	85
Pump isentropic efficiency	η_P (%)	90
Pinch point temperature difference	ΔT_{PP} (°C)	5
Interest rate	i_r (%)	10
Plant economic life	n (year)	20
Annual operating hours	τ (h)	7500

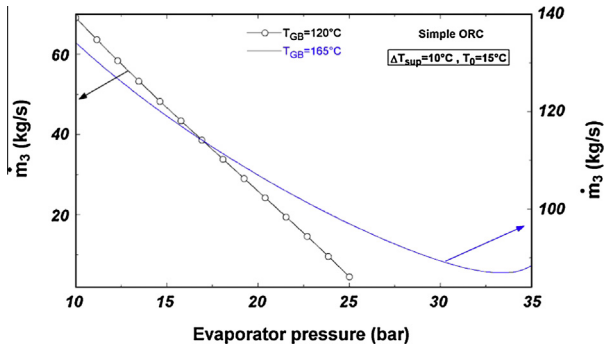

Fig. 5. Effects on the working fluid mass flow rate of evaporator pressure for different heat source temperatures.

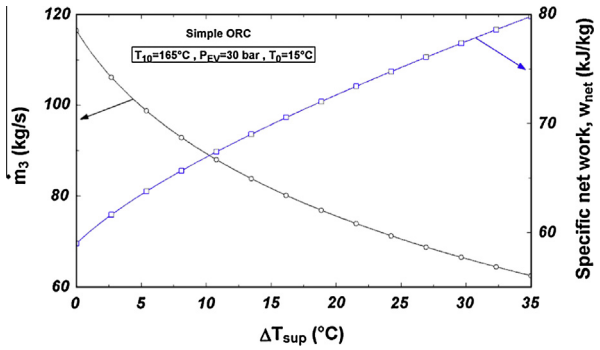

Fig. 7. Effects on the working fluid mass flow rate and specific net work of vapor superheating degree at turbine inlet.

then increases slightly, so that it can be minimized at a special value of ΔT_{sup}. Such a trend of $\dot{C}_{P,total}$ is mainly due to the variations of costs of the evaporator and the superheater. It can be argued that, an increase of ΔT_{sup} decreases the amount of transferred heat in the evaporator which brings about a reduction in its size and cost. However, it is clear that increasing ΔT_{sup} results in an increase of the superheater's size and cost. A reduced value of $\dot{Z}_{EV}$ and an increased value of $\dot{Z}_{Sup}$ bring about the trend presented in Fig. 6(b) for $\dot{C}_{P,total}$. Also, Fig. 6(a) indicates that, as ΔT_{sup} increases, the net output power decreases. This trend can be justified regarding the variations of working fluid mass flow rate and the specific net work presented in Fig. 7. As can be seen, an increase in ΔT_{sup} decreases the working fluid mass flow rate (because of a lower heat absorption in the evaporator) while the increase in specific net work cannot compensate the reduction of mass flow rate, considering the relation: $\dot{W}_{net} = \dot{m}_3 w_{net}$.

The variations of the total product cost and net output power of the cycles with condenser temperature are shown in Fig. 8(a and b). Referring to Fig. 8(a and b), increasing the condenser temperature results in a significant decrease of $\dot{W}_{net}$ and an slight decrease of $\dot{C}_{P,total}$. The reduction of $\dot{C}_{P,total}$ is mainly due to the reduction of turbine's size and cost as it generates less power with a higher condenser temperature.

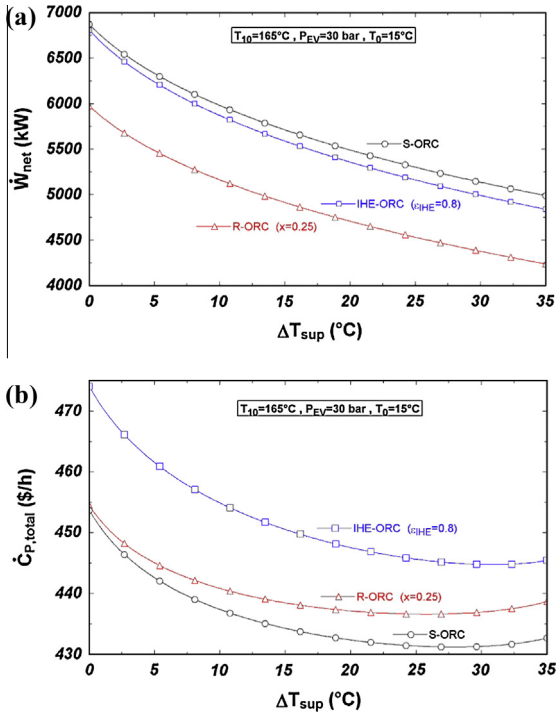

Fig. 6. Effects on the total product cost and net output power of vapor superheating degree at turbine inlet.

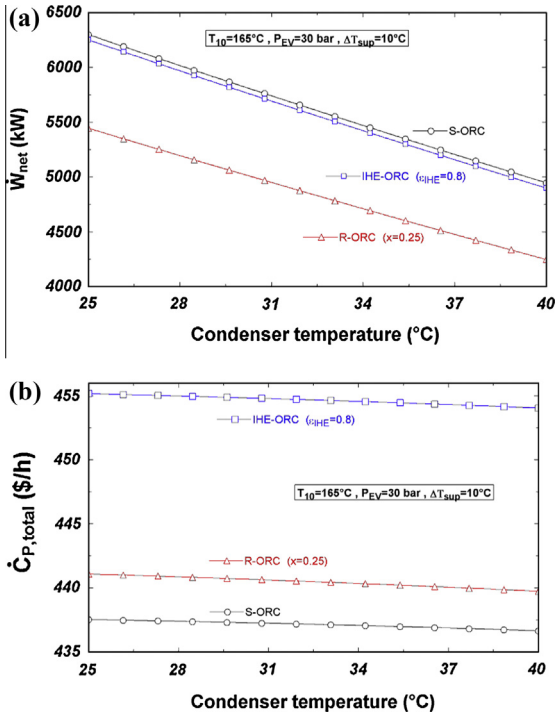

Fig. 8. Effects on the total product cost and net output power of condenser temperature.

The effects of the pinch point temperature difference on the total product cost and the net output power of the considered cycles are shown in Fig. 9(a and b). As the figure indicates, lower values of $\dot{W}_{net}$ and $\dot{C}_{P,total}$ are obtained for higher ΔT_{PP}. The reduction of net output power is due to the fact that as ΔT_{PP} increases the mass flow rate of organic fluid decreases because of a lower evaporator heat duty. A lower evaporator and condenser heat duty as a result of increasing ΔT_{PP} brings about a lower heat transfer area and hence a lower cost for these components. This is the main reason why $\dot{C}_{P,total}$ decreases with increasing ΔT_{PP}.

Two important parameters (except than those investigated above) that influence the IHE-ORC and R-ORC performances are IHE effectiveness and the ratio of extracted vapor from turbine

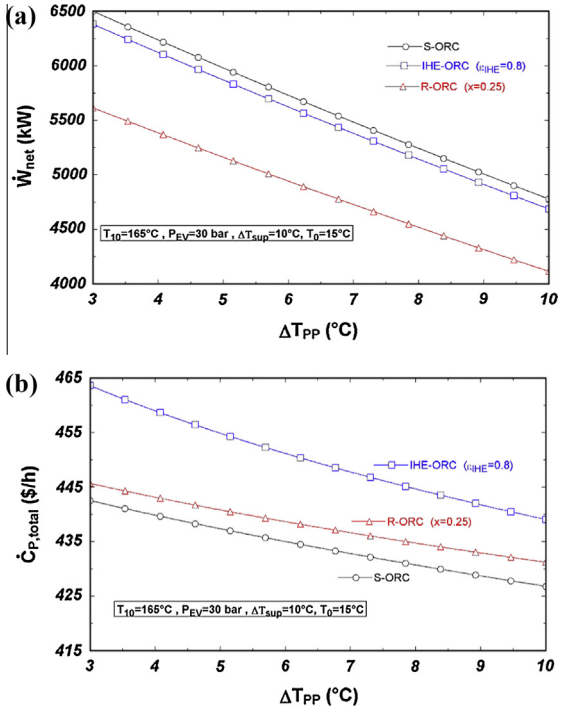

Fig. 9. Effects on the total product cost and net output power of pinch point temperature difference.

for feed heater. The effects of the IHE effectiveness on the total product cost and the net output power of the IHE-ORC are depicted in Fig. 10. Referring to Fig. 10, higher $\dot{C}_{P,total}$ values are obtained for higher IHE effectiveness which is due to a higher heat transfer area and purchased equipment cost for IHE.

Fig. 11 shows the variations of total product cost and net output power of the R-ORC with the ratio of extracted vapor ($x = \dot{m}_7/\dot{m}_3$) entering the feed heater. As the figure indicates, increasing the extracted vapor ratio results in a decrease in $\dot{W}_{net}$ and $\dot{C}_{P,total}$. The decrease of $\dot{C}_{P,total}$ is mainly due to a reduction in turbine and condenser sizes and costs as the x increases.

5.2. Results of exergoeconomic optimization

The cycles' performances are optimized for minimum total product cost. The objective function and the constraints are as follows:

$$\text{Minimize } \dot{C}_{P,total}(P_{EV}, T_{CD}, \Delta T_{PP}, \Delta T_{sup}, \varepsilon_{IHE}, x) \tag{21}$$

Subjected to constraints:

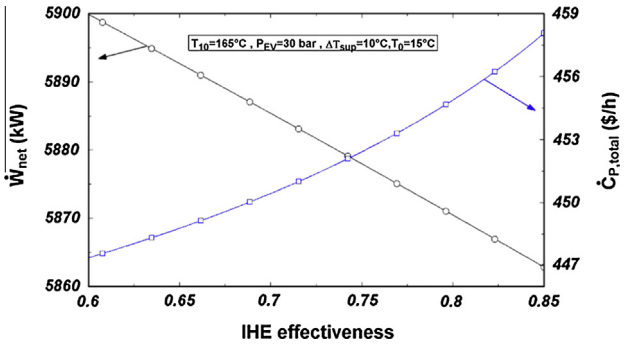

Fig. 10. Effects on the total product cost and net output power of IHE effectiveness.

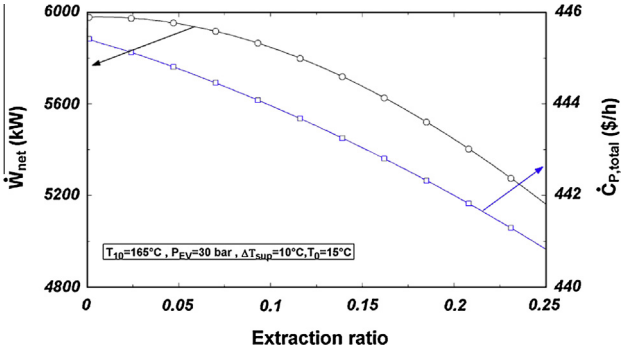

Fig. 11. Effects on the total product cost and net output power of extracted vapor ratio.

$$\begin{aligned} &15 < P_{EV}(bar) < 35 \\ &25 < T_{CD}(^{\circ}\mathrm{C}) < 40 \\ &3 < \Delta T_{PP}(^{\circ}\mathrm{C}) < 10 \\ &60 < \varepsilon_{IHE}(\%) < 85 \\ &0 < x < 0.25 \\ &0 < \Delta T_{sup}(^{\circ}\mathrm{C}) < 50 \end{aligned} \tag{22}$$

The direct search method is selected for optimizing the cycles' performances. This method is deemed suitable for problems involving simulation-based optimization or optimizing non-numerical functions [37]. The direct search method employs a successive search to find an extremum by directly comparing objective function values at a sequence of trial points without involving derivatives.

For the Isobutane as the working fluid, the optimization results are outlined in Table 7 for different geothermal brine temperatures. As the Table indicates, for a given heat source temperature, the S-ORC has the lowest value of $\dot{C}_{P,total}$ among the considered cycles. Also, this configuration has the highest value of net output power. In addition, the values of first and second law efficiencies for the IHE-ORC are higher than those for two other cases. A lower reinjection temperature for S-ORC indicates that this cycle can utilize more energy and exergy of the geothermal heat source than the other cycles.

Referring to figures given in Table 7, it is revealed that from the thermodynamic point of view (thermal and exergy efficiencies), the ORC-IHE has the best performance while from the exergoeconomic viewpoint the S-ORC is the best case. The superiority of ORC-IHE over the other configurations, from the thermodynamic viewpoint, is also reported previously by Yari in a comprehensive thermodynamic analysis [9].

For other working fluids, the results of optimization are outlined in Table 8 for the base case geothermal brine temperature of 165 °C. As the Table indicates, employing n-pentane as the working fluid brings about higher values of first and second law efficiencies and lower values of $\dot{C}_{P,total}$ compared to the other working fluids. A lower $\dot{C}_{P,total}$ is mainly due to a lower mass flow rate of the working fluid which results in lower components' sizes and costs. A lower mass flow rate of the working fluid is in turn caused by a higher latent heat of the n-pentane. A lower mass flow rate of the working fluid, also results in a lower net output power for n-pentane as Table 8 indicates. However, a higher value of the first and second law efficiencies for n-pentane is due to the fact that the utilized geothermal heat is lower since the reinjection temperature for this working fluid is higher.

As an important criterion in exergoeconomic assessment in component level is the exergy destruction cost rate, $\dot{C}_{D,k}$. For component k, this parameter is defined as [29]:

Table 7
Optimization results for minimum $\dot{C}_{P,total}$ for Isobutane as the working fluid.

Decision variables/performance parameters	Different configurations of ORCs								
	S-ORC			ORC-IHE			R-ORC		
T_{GB} (°C)	160	165	170	160	165	170	160	165	170
Evaporator pressure (bar)	32.88	30.25	26.21	33.29	31.03	28.15	31.79	25.91	15.01
Degree of supearheat (°C)	20.59	26.98	36.09	20.18	27.68	35.51	19.52	29.82	40.19
Condenser temperature (°C)	40	40	40	40	40	40	40	40	40
Pinch point temperature difference (°C)	10	10	10	10	10	10	10	10	10
IHE effectiveness	–	–	–	0.60	0.60	0.60	–	–	–
Extracted vapor ratio	–	–	–	–	–	–	0.25	0.25	0.25
$\dot{C}_{P,total}$ ($/h)	417.4	421.9	425.2	422.5	427.7	431.6	424.3	427.6	428.2
$\dot{W}_{net}$ (kW)	3016	3703	4230	2960	3631	4171	2690	3249	2897
η_I (%)	13.51	13.11	12.31	15.33	15.23	14.90	14.96	13.52	8.89
η_{II} (%)	49.41	48.77	46.73	54.29	54.14	53.03	52.94	48.69	33.19
$T_{GB,out}$ (°C)	107.8	98.93	89.56	114.9	109.3	104.7	118.0	108.9	93.75

Table 8
Optimization results for different working fluids.

Working fluid	R245fa			n-pentane			R152a		
Decision variables/performance parameters	S-ORC	IHE-ORC	R-ORC	S-ORC	IHE-ORC	R-ORC	S-ORC	IHE-ORC	R-ORC
Evaporator pressure (bar)	27.01	22.54	20.54	14.47	13.75	14.12	18.47	22.54	24.12
Degree of supearheat (°C)	4.76	11.67	22.74	10.19	4.06	0	30.74	41.67	34.74
Condenser temperature (°C)	40	40	40	40	40	40	40	40	40
Pinch point temperature difference (°C)	10	10	10	10	10	10	10	10	10
IHE effectiveness	–	0.6	–	–	0.6	–	–	0.6	–
Extracted vapor ratio	–	–	0.25	–	–	0.25	–	–	0.25
$\dot{C}_{P,total}$ ($/h)	409.7	419.5	422.5	393.8	399.7	409.7	427.8	436.0	430.1
$\dot{W}_{net}$ (kW)	2840	3415	2910	1449	1723	1479	2967	3536	2794
η_I (%)	14.61	15.20	14.97	15.49	17.18	17.45	6.68	9.22	8.88
η_{II} (%)	50.24	53.26	51.93	50.22	55.47	56.22	28.75	37.01	33.65

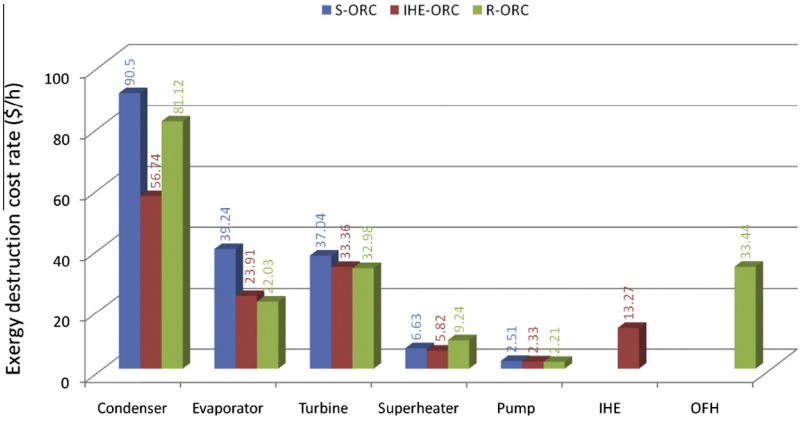

Fig. 12. The values of exergy destruction cost rates for cycles' components at T_{GB} = 165 °C.

$$\dot{C}_{D,k} = c_{F,k}\dot{E}_{D,k} \tag{23}$$

For the components of three considered ORCs, the values of $\dot{C}_{D,k}$, under the optimized operating conditions (for Isobutane as the working fluid), are presented in Fig. 12. Referring to Fig. 12, it is revealed that, in all the three cycles, condenser and turbine have higher values of exergy destruction cost rates compared to the other components. Also, it is seen that in regenerative organic Rankine cycle, the open feed heater (OFH) has a relativity high value of $\dot{C}_{D,k}$.

6. Profitability evaluation of different cycles

It is of economic importance to reduce the total capital investment per installed kW for a geothermal power plant. The investment costs of geothermal power plants can be divided into two categories: surface equipment (the plant component costs) and subsurface investments (drilling the wells) [32]. For the investigated cycles in the present study, the total capital investment per unit output power, under the optimized conditions, is presented in Fig. 13. Referring to Fig. 13, at a given heat source temperature, the S-ORC has lower TCI values than two other cases. For a heat source temperature of 165 °C for instance, the TCI value for the S-ORC is 10.2% and 22.9% lower than that for IHE-ORC and R-ORC, respectively.

Another criterion for profitability evaluation is the payback period defined as the time required for the amount invested in an asset to be repaid by the net cash inflow. The payback period for the capital investment is defined as [38]:

$$PP = \frac{\mathrm{TCI}}{\mathrm{AR}} \tag{24}$$

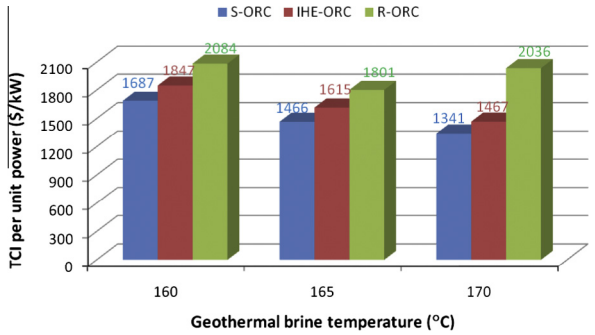

Fig. 13. The total capital investment per unit output power at different heat source temperatures.

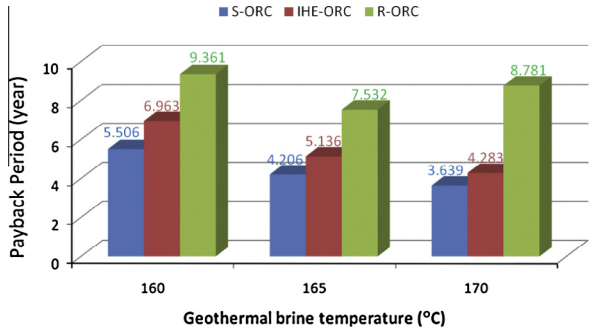

Fig. 14. The payback periods at different heat source temperatures.

where the TCI is the total capital investment and the AR is the annual revenue which is gained from the product sale incomes. For the considered cycles, the payback periods, under the optimized conditions, are presented in Fig. 14. As the figure indicates, the S-ORC has the shortest payback period. This is due to the fact that the S-ORC has the highest value of output power (see Table 7) and the lowest value of TCI (see Fig. 13).

7. Conclusions

A comprehensive exergoeconomic analysis, optimization and performance comparison is reported of three ORC configurations for binary geothermal power plants. The considered objective function is the total product cost minimization. A comparison between the investigated systems, at the optimum operating conditions, revealed the following findings:

1. The simple ORC has the highest value of net output power.
2. The highest values of first and second law efficiencies correspond to the ORC with internal heat exchanger.
3. The simple ORC has the lowest value of the total product cost.
4. Among the considered working fluids, n-pentane yields the highest first and second law efficiencies as well as the lowest total product cost.
5. The lowest total capital investment and the shortest payback period are associated with the simple ORC.

References

[1] Astolfi M, Xodo L, Romano MC, Macchi E. Technical and economical analysis of a solar–geothermal hybrid plant based on an Organic Rankine Cycle. Geothermics 2011;40:58–68. http://dx.doi.org/10.1016/j.geothermics.2010.09.009.

[2] DiPippo R, Moya P. Las Pailas geothermal binary power plant, Rincón de la Vieja, Costa Rica: performance assessment of plant and alternatives. Geothermics 2013;48:1–15. http://dx.doi.org/10.1016/j.geothermics.2013.03.006.

[3] Unverdi M, Cerci Y. Performance analysis of Germencik geothermal power plant. Energy 2013;52:192–200. http://dx.doi.org/10.1016/j.energy.2012.12.052.

[4] Aneke M, Agnew B, Underwood C. Performance analysis of the Chena binary geothermal power plant. Appl Therm Eng 2011;31:1825–32. http://dx.doi.org/10.1016/j.applthermaleng.2011.02.028.

[5] Luo C, Huang L, Gong Y, Ma W. Thermodynamic comparison of different types of geothermal power plant systems and case studies in China. Renew Energy 2012;48:155–60. http://dx.doi.org/10.1016/j.renene.2012.04.037.

[6] DiPippo R. Second law assessment of binary plants generating power from low-temperature geothermal fluids. Geothermics 2004;33:565–86. http://dx.doi.org/10.1016/j.geothermics.2003.10.003.

[7] Kanoglu M, Bolatturk A. Performance and parametric investigation of a binary geothermal power plant by exergy. Renew Energy 2008;33:2366–74. http://dx.doi.org/10.1016/j.renene.2008.01.017.

[8] Madhawa Hettiarachchi HD, Golubovic M, Worek WM, Ikegami Y. Optimum design criteria for an Organic Rankine cycle using low-temperature geothermal heat sources. Energy 2007;32:1698–706. http://dx.doi.org/10.1016/j.energy.2007.01.005.

[9] Yari M. Exergetic analysis of various types of geothermal power plants. Renew Energy 2010;35:112–21. http://dx.doi.org/10.1016/j.renene.2009.07.023.

[10] Astolfi M, Romano MC, Bombarda P, Macchi E. Binary ORC (Organic Rankine Cycles) power plants for the exploitation of medium–low temperature geothermal sources – Part B: Techno-economic optimization. Energy 2014;66:423–34. http://dx.doi.org/10.1016/j.energy.2013.11.056.

[11] Walraven D, Laenen B, D'haeseleer W. Comparison of thermodynamic cycles for power production from low-temperature geothermal heat sources. Energy Convers Manage 2013;66:220–33. http://dx.doi.org/10.1016/j.enconman.2012.10.003.

[12] Ganjehsarabi H, Gungor A, Dincer I. Exergoeconomic evaluation of a geothermal power plant. Int J Exergy 2014;14:303–19.

[13] Heberle F, Bassermann P, Preißinger M, Brüggemann D. Exergoeconomic optimization of an Organic Rankine Cycle for low-temperature geothermal heat sources. Int J Thermodyn 2012;15:119–26. http://dx.doi.org/10.5541/ijot.374.

[14] Ghasemi H, Paci M, Tizzanini A, Mitsos A. Modeling and optimization of a binary geothermal power plant. Energy 2013;50:412–28. http://dx.doi.org/10.1016/j.energy.2012.10.039.

[15] Zhang SJ, Wang H, Gou T. Performance comparison and parametric optimization of subcritical Organic Rankine Cycle (ORC) and transcritical power cycle system for low-temperature geothermal power generation. Appl Energy 2011;88:2740–54. http://dx.doi.org/10.1016/j.apenergy.2011.02.034.

[16] Xiaomin L, Xing W, Chuhua Z. Sensitivity analysis of system parameters on the performance of the Organic Rankine Cycle system for binary-cycle geothermal power plants. Appl Therm Eng 2014;71:175–83. http://dx.doi.org/10.1016/j.applthermaleng.2014.06.048.

[17] Fu-Zhen Z, Pei-Xue J. Thermodynamic analysis of a binary power cycle for different EGS geofluid temperatures. Appl Therm Eng 2012;48:476–85. http://dx.doi.org/10.1016/j.applthermaleng.2012.04.028.

[18] El-Emam RS, Dincer I. Exergy and exergoeconomic analyses and optimization of geothermal organic Rankine cycle. Appl Therm Eng 2013;59:435–44. http://dx.doi.org/10.1016/j.applthermaleng.2013.06.005.

[19] Imran M, Park BS, Kim HJ, Lee DH, Usman M, Heo M. Thermo-economic optimization of Regenerative Organic Rankine Cycle for waste heat recovery applications. Energy Convers Manage 2014;87:107–18. http://dx.doi.org/10.1016/j.enconman.2014.06.091.

[20] Franco A. Power production from a moderate temperature geothermal resource with regenerative Organic Rankine Cycles. Energy Sustain Dev 2011;15:411–9. http://dx.doi.org/10.1016/j.esd.2011.06.002.

[21] Maoqing L, Jiangfeng W, Weifeng H, Lin G, Bo W, Shaolin M, et al. Construction and preliminary test of a low-temperature regenerative Organic Rankine Cycle (ORC) using R123. Renew Energy 2013;57:216–22. http://dx.doi.org/10.1016/j.renene.2013.01.042.

[22] Schuster A, Karellas S, Kakaras E, Spliethoff H. Energetic and economic investigation of Organic Rankine Cycle applications. Appl Therm Eng 2009;29:1809–17. http://dx.doi.org/10.1016/j.applthermaleng.2008.08.016.

[23] Cong G, Xiaoze D, Lijun Y, Yongping Y. Performance analysis of organic Rankine cycle based on location of heat transfer pinch point in evaporator. Appl Therm Eng 2014;62:176–86. http://dx.doi.org/10.1016/j.applthermaleng.2013.09.036.

[24] Franco A, Villani M. Optimal design of binary cycle power plants for water-dominated, medium-temperature geothermal fields. Geothermics 2009;38:379–91. http://dx.doi.org/10.1016/j.geothermics.2009.08.001.

[25] Hung TC, Wang SK, Kuo CH, Pei BS, Tsai KF. A study of organic working fluids on system efficiency of an ORC using low-grade energy sources. Energy 2010;35:1403–11. http://dx.doi.org/10.1016/j.energy.2009.11.025.

[26] Huixing Z, Lin S, Qingsong A. Influence of working fluid properties on system performance and screen evaluation indicators for geothermal ORC (organic Rankine cycle) system. Energy 2014;74:2–11. http://dx.doi.org/10.1016/j.energy.2013.12.030.

[27] Fubin Y, Xiaorui D, Hongguang Z, Zhen W, Kai Y, Jian Z, et al. Performance analysis of waste heat recovery with a dual loop organic Rankine cycle (ORC)

system for diesel engine under various operating conditions. Energy Convers Manage 2014;80:243–55. http://dx.doi.org/10.1016/j.enconman.2014.01.036.
[28] Lazzaretto A, Tsatsaronis G. SPECO: a systematic and general methodology for calculating efficiencies and costs in thermal systems. Energy 2006;31:1257–89. http://dx.doi.org/10.1016/j.energy.2005.03.011.
[29] Bejan A, Tsatsaronis G, Moran M. Thermal design and optimization. New York: John Wiley and Sons Inc.; 1996.
[30] Zare V, Mahmoudi SMS, Yari M. On the exergoeconomic assessment of employing Kalina cycle for GT-MHR waste heat utilization. Energy Convers Manage 2015;90:364–74. http://dx.doi.org/10.1016/j.enconman.2014.11.039.
[31] Calise F, Capuozzo C, Carotenuto A, Vanoli L. Thermoeconomic analysis and off-design performance of an organic Rankine cycle powered by medium-temperature heat sources. Sol Energy 2014;103:595–609. http://dx.doi.org/10.1016/j.solener.2013.09.031.
[32] Stefansson V. Investment cost for geothermal power plants. Geothermics 2002;31:263–72.
[33] Yari M, Mehr AS, Zare V, Mahmoudi SMS, Rosen MA. Exergoeconomic comparison of TLC (trilateral Rankine cycle), ORC (organic Rankine cycle) and Kalina cycle using a low grade heat source. Energy 2015;83:712–22. http://dx.doi.org/10.1016/j.energy.2015.02.080.
[34] Paulus DM, Tsatsaronis G. Auxiliary equations for the determination of specific exergy revenues. Energy 2006;31:3235–47. http://dx.doi.org/10.1016/j.energy.2006.03.003.
[35] Ghaebi H, Saidi MH, Ahmadi P. Exergoeconomic optimization of a trigeneration system for heating, cooling and power production purpose based on TRR method and using evolutionary algorithm. Appl Therm Eng 2012;36:113–25. http://dx.doi.org/10.1016/j.applthermaleng.2011.11.069.
[36] Ahmadi P, Dincer I, Rosen MA. Thermodynamic modeling and multi-objective evolutionary-based optimization of a new multigeneration energy system. Energy Convers Manage 2013;76:282–300. http://dx.doi.org/10.1016/j.enconman.2013.07.049.
[37] Zare V, Yari M, Mahmoudi SMS. Proposal and analysis of a new combined cogeneration system based on the GT-MHR cycle. Desalination 2012;286:417–28. http://dx.doi.org/10.1016/j.desal.2011.12.001.
[38] Zare V, Mahmoudi SMS, Yari M. An exergoeconomic investigation of waste heat recovery from the Gas Turbine-Modular Helium Reactor (GT-MHR) employing an ammonia–water power/cooling cycle. Energy 2013;61:397–409. http://dx.doi.org/10.1016/j.energy.2013.09.038.